Muon-spin-rotation measurements in infinite-layer and infinite-chain cuprate antiferromagnets: $Ca_{0.86}Sr_{0.14}CuO_2$ and Sr_2CuO_3

A. Keren, L. P. Le, G. M. Luke, B. J. Sternlieb,* W. D. Wu, and Y. J. Uemura

Department of Physics, Columbia University, New York, New York 10027

S. Tajima

Superconductivity Research Laboratory, International Superconductivity Technology Center, 1-10-13, Shinonome, Koto-ku, Tokyo 135, Japan

S. Uchida

Department of Applied Physics, Faculty of Engineering, University of Tokyo, Bunkyo-ku, Tokyo 113, Japan

(Received 23 April 1993)

We have performed zero-field muon-spin-rotation measurements of the "infinite-layer" cuprate compound $Ca_{0.86}Sr_{0.14}CuO_2$ and the "infinite-chain" system Sr_2CuO_3. A spontaneous magnetic field from the ordered Cu moments is observed below $T_N = 540 \pm 5$ K in $Ca_{0.86}Sr_{0.14}CuO_2$: below $T = 360$ K, we observe muon-spin precession with a frequency $\nu(T \to 0) = 16$ MHz (corresponding to a local field of 1.2 kG). The precession signal is replaced by a rapid depolarization above $T = 360$ K due to the onset of muon diffusion. The hopping rate followed an Arrhenius law, with an activation energy of $E_a = 0.39(1)$ eV. The sublattice magnetization M_s, proportional to $\nu(T)$, showed a slower decay with increasing temperature in $Ca_{0.86}Sr_{0.14}CuO_2$, compared with that observed in La_2CuO_4 and $Sr_2CuO_2Cl_2$, indicating that a wider CuO_2-layer separation results in more two-dimensional magnetic behavior. In the infinite-chain system Sr_2CuO_3, the onset of magnetic order was found at $T \sim 5$ K with a local field of ~ 30 G at the muon site at $T \to 0$. The exchange interaction, inferred from susceptibility measurements is on the order of 10^3 K, implying a remarkable suppression of the ordering temperature with $k_B T_N / J \leq 0.01$ in Sr_2CuO_3. These results demonstrate clear signatures of low-dimensional magnetic behavior in the CuO chains.

I. INTRODUCTION

The discovery of high-temperature superconductivity in cuprate systems has generated considerable interest in the magnetic properties of their undoped parent compounds.[1] This is partly based on the widely accepted conjecture that the superconductivity of the high-T_c cuprates is intimately related to the magnetic interactions within the CuO_2 planes. Another source of interest comes from the fact that some of the parent antiferromagnets, such as La_2CuO_4, represent nearly ideal two-dimensional Heisenberg spin systems.[2] The so-called 1:2:3 compound $YBa_2Cu_3O_7$ is perhaps the most extensively studied among the various cuprates. The 1:2:3 system has a layered perovskite structure, shown in Fig. 1, with three copper-oxygen layers stacked along the tetragonal $\hat{c}$ axis. Two of these layers have oxygen ions between the copper ions in both the $\hat{a}$ and $\hat{b}$ directions, and thus are called CuO_2 plane layers. The third layer, called the CuO chain layer, has oxygen ions only along the $\hat{b}$ axis: $YBa_2Cu_3O_y$ with $y = 7.0$ has complete CuO chains, while some oxygen atoms are missing and the chains are fragmental for materials with $y < 7.0$. Since the CuO_2 plane and the CuO chain represent two important building blocks of high-T_c cuprate compounds, it is useful to study their magnetic behavior separately.

In this paper we examine the magnetic properties of two different systems, $Ca_{0.86}Sr_{0.14}CuO_2$ and Sr_2CuO_3, using the muon-spin-rotation (μSR) technique. $Ca_{0.86}Sr_{0.14}CuO_2$, with the structure shown in Fig. 1, is characterized by the highest density of the CuO_2 planes among the various cuprate systems, with no other layers sandwiched between the CuO_2 planes.[3] Systems with this structure are often called "infinite layer" (IL) compounds. Recently, superconducting IL systems, with T_c's up to 110 K, have been synthesized under high pressure.[4] $Ca_{0.86}Sr_{0.14}CuO_2$ as studied here is the undoped parent antiferromagnetic system of these IL superconductors.
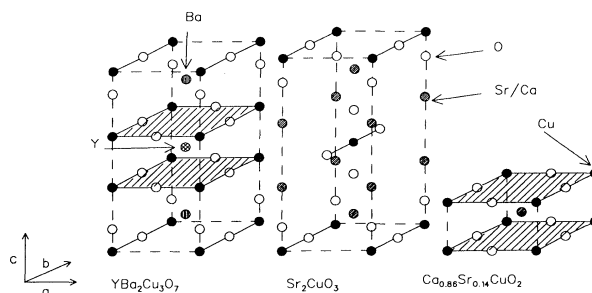

FIG. 1. Crystal structures of $YBa_2Cu_3O_7$, Sr_2CuO_3, and $Ca_{0.86}Sr_{0.14}CuO_2$. The exchange couplings along layers and chains are emphasized by the solid lines.

Antiferromagnetic order in this system, with Néel temperature $T_N = 537 \pm 5$ K, was first confirmed by neutron scattering measurements.[5]

The so-called "infinite-chain" (IC) system, Sr_2CuO_3, has a structure resembling the chain layer of the 1:2:3 system, as shown in Fig. 1. The structure of this system could lead to a strongly one-dimensional (1D) magnetic interaction. Chemical charge counting arguments suggest that Sr_2CuO_3 has CuO chains without free charge carriers. No information has been available on possible magnetic ordering in Sr_2CuO_3, except for the fact that two-magnon Raman scattering was not seen in this system at room temperature.[6] Comparison of these two systems could help us understand the role of dimensionality in the magnetic properties of cuprates.

In addition to studies of various intrinsic magnetic properties, we also present results on the muon site and diffusion in the IL system. The simplicity of its crystal structure makes this system nearly ideal for such studies. $Ca_{0.86}Sr_{0.14}CuO_2$ orders magnetically at a temperature high enough for muons to hop between interstitial sites within the antiferromagnetically ordered state. We can study the temperature dependence of the hopping rate via the fast dephasing of the muon-spin precession, using a phenomenological treatment described in the Appendix. Results on the diffusion rate may be compared with models involving the electrostatic potential at the muon site. In order to look for possible muon sites in an IL, we compare the muon-spin-rotation frequency observed at low temperatures with a model calculation for the local field assuming a dipolar interaction.

This paper is organized as follows: Principles of the μSR technique and various experimental aspects are described in Sec. II. In Sec. III we present μSR results on $Ca_{0.86}Sr_{0.14}CuO_2$ and compare them with neutron scattering measurements.[5] Discussions of muon diffusion and muon sites in this system are given in Sec. IV. μSR measurements of Sr_2CuO_3 are presented in Sec. V. In Sec. VI we present dc-susceptibility measurements of $Ca_{0.86}Sr_{0.14}CuO_2$ and Sr_2CuO_3, and compare them with the observed susceptibility in other layered compounds, as well as to a model calculation for a Heisenberg spin chain. In Sec. VII we compare the present results in $Ca_{0.86}Sr_{0.14}CuO_2$ with previous μSR results for La_2CuO_4,[7] $Sr_2CuO_2Cl_2$,[2] and discuss differences in their magnetic properties within the framework of a quasi-two-dimensional Heisenberg model. Implications of the present results on the magnetic properties of the 1:2:3 system will also be discussed: We point out that Sr_2CuO_3 may serve as a parent insulating material for hole-doped 1D CuO chains, a possible realization of a one-dimensional Hubbard model. In the Appendix, a strong collision model is applied to describe muon diffusion in an antiferromagnet.

II. μSR EXPERIMENTAL SETUP

In a μSR experiment[8,9] a beam of polarized positive muons is focused on a specimen (typically 10 mm $\times$ 10 mm $\times$ 2–3 mm) mounted in a cryostat or oven. Each im-

planted muon stops almost instantaneously (within less than 10^{-10} s) at an interstitial site. The muon subsequently decays (with a mean lifetime $\tau_\mu = 2.2$ μs), emitting a decay positron preferentially along the muon-spin direction. A time histogram of more than 10^6 muon decay events are obtained, event by event, using a muon defining counter which creates a clock-start pulse at the arrival of a μ^+ into the specimen, and two positron detectors [placed forward (+) and backward (−) with respect to the initial muon-spin direction] which create a clock-stop pulse. In zero field (ZF), the expected time histograms of the positrons from the opposing counters are given as

$$N^{\pm}(t) = N_0^{\pm} \exp(-t/\tau_\mu)[1 \pm AG_z(t)] , \qquad (1)$$

where A is initial asymmetry, and $G_z(t)$ is the muon-spin relaxation function along the direction of its initial spin polarization. The corrected asymmetry $AG_z(t)$ can then be obtained:

$$AG_z(t) = \frac{N^+ - \alpha N^-}{N^+ + \alpha N^-} , \qquad (2)$$

where $\alpha = N^+(0)/N^-(0)$ is a factor related to the difference in effective solid angles of the two detectors.

The muon spin precesses in the local internal field at an angular frequency $\omega = \gamma_\mu H_{\text{loc}}$ ($\gamma_\mu = 85.162$ MHz/kG). The relaxation function $G_z(t)$ describes the time evolution of the muon polarization. In the paramagnetic state of a magnetic system, $G_z(t)$ in zero field usually has a simple form $G_z(t) = \exp(-t/T_1) \times G_z^{\text{ND}}(t)$, where the exponential term represents the effect of fluctuating local fields from paramagnetic moments. In the "narrowing limit," where the fluctuation rate ν_p of the local field is much larger than the frequency $\omega = \gamma_\mu H_{\text{loc}}$ due to the instantaneous local field, the spin-lattice relaxation time T_1 is given as $1/T_1 = \omega^2/\nu_p$. $G_z^{\text{ND}}(t)$ is the relaxation function due to nuclear dipolar fields; in zero field and the static case, $G_z^{\text{ND}}(t)$ is given by the Kubo-Toyabe function.[8]

In the ordered state of a randomly oriented sample, the zero-field relaxation function $G_z(t)$ is given by

$$G_z(t) = \frac{1}{3} \exp(-t/T_1)$$
$$+ \frac{2}{3} \exp\left(\frac{-\sigma^2 t^2}{2}\right) \exp(-t/T_2) \cos(\omega t) , \qquad (3)$$

where the 1/3 (2/3) component is due to muons stopped at a site where the local field is parallel (perpendicular) to the initial spin polarization. The 1/3 term selectively reflects the dynamic modulation of the local fields, whereas the 2/3 component reflects both the dynamic effect and the static inhomogeneity of the local field H_{loc} from the ordered moments. When the nuclear dipolar field is the only source of inhomogeneity in the static local field, we can express the transverse spin depolarization as a product of two terms: $\exp(-t/T_2)$ representing the dynamic effect and the Gaussian damping $\exp(-\frac{1}{2}\sigma^2 t^2)$ due to static nuclear dipolar fields. At temperatures where muon hopping takes place, dynamic changes of the lo-

cal field due to the muon motion becomes a significant cause of relaxation. In the Appendix, we derive an expression for the relaxation function in the ordered state of an antiferromagnet when the muon hops at a rate ν_h between sites having local fields in opposite directions. For a unique crystallographic site occupancy, $G_z^h(t)$ is given by

$$G_z^h(t) = \frac{1}{3}e^{-t/T_1} + \frac{2}{3}e^{-t/T_2}(c_+e^{z_+t} + c_-e^{z_-t}), \quad (4)$$

where

$$c_\pm = \frac{1}{2} \pm \frac{\nu_h(\nu_h^2 - \omega^2)^{-\frac{1}{2}}}{2}$$

and

$$z_\pm = -\nu_h \pm (\nu_h^2 - \omega^2)^{\frac{1}{2}}.$$

The 1/3 component is not influenced by hopping in this model. This component is due to muons that stop in a site with the local field pointing along their spin direction. These muons will not precess in the local field before or after the hop, and so their spin will not depolarize as a result of the hop.

For both fast ($\nu_h > \omega$) and slow ($\nu_h < \omega$) hopping, the relaxation of the 2/3 component at $t \ll 2\pi/\omega$, follows t as $1 - (1/2)\omega^2t^2$. This quadratic behavior at $t \to 0$ is expected in a strong collision model. At long times $t \gg 2\pi/\omega$, two limits are of interest: In the very fast hopping limit ($\nu \gg \omega$) the 2/3 component relaxation function is given by $\exp(-\omega^2t/2\nu)$, as in the narrowing limit of a paramagnetic state. In the very slow hopping limit $\nu \ll \omega$, the time dependence of the 2/3 component goes as $\exp(-\nu t)\cos(\omega t)$. In this limit, the relaxation rate can be understood by noting that only the spins of muons that have not hopped at all will contribute to the polarization at long times; the number of such muons decreases exponentially.

which were finally sintered at 980 °C for 12 h. The specimen was checked by x-ray diffraction; we could not find any impurity peak with an intensity greater than 1% of the (011)-peak height of the IL structure.

The μSR experiments were performed at the M15 surface muon channel at TRIUMF. Several pieces of sintered polycrystalline specimens, each approximately $5 \times 5 \times 0.5$ mm^3, were mounted in a He gas flow cryostat which operates in a temperature region from 3.0 to 300 K. An oven was used to obtain higher temperatures. Figure 2 shows typical time spectra of the muon polarization observed in Ca$_{0.86}$Sr$_{0.14}$CuO$_2$ between 400 K and 545 K. A large increase in the muon-spin depolarization rate is seen between 545 K and 535 K. The relaxation at 545 K is characteristic of nuclear magnetic moments whereas the relaxation at 535 K is due to the freezing of electronic moments. The Néel temperature $T_N = 540 \pm 5$ K, estimated from Fig. 2, is in very good agreement with $T_N = 537 \pm 5$ K found in neutron scattering measurements.[5] Another indication of magnetic order comes from magnon Raman scattering at room temperature in which a fairly strong but broad Raman band around 3000 cm^{-1} has been attributed to spin-pair (two-magnon) excitations.[13]

Figure 3 shows time spectra at 102, 245, and 360 K. At 102 K and 245 K spin precession is evident and the signal has a characteristic exponential decay. This indicates the existence of static magnetic order at those temperatures. Fourier transforms of the spectra at two temperatures are shown in the inset of Fig. 4. At 102 K, two frequencies are present, but only one frequency exists at 245 K. Such a splitting of the precession frequency was also seen in Sr$_2$CuO$_2$Cl$_2$ and can be the result of either a unique muon site that lacks the symmetry of the magnetic system, or two different muon sites both having the symmetry of the magnetic system. Muon hopping, with a rate increasing with increasing temperature, can then be responsible for the merging of the two frequen-
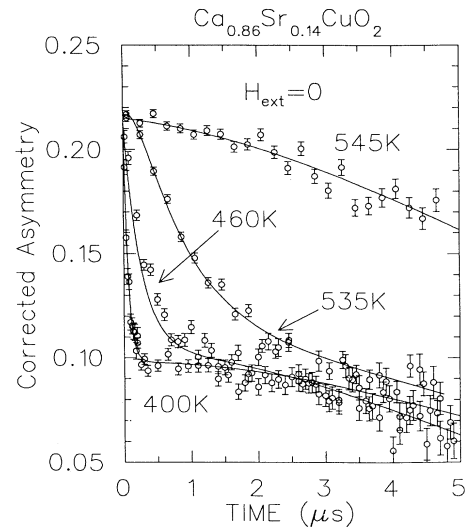
III. μSR IN Ca$_{0.86}$Sr$_{0.14}$CuO$_2$

The first infinite layer material was reported by Roth.[10] At ambient pressure the structure of Sr$_{1-x}$Ca$_x$CuO$_2$ can only be stabilized with $x \sim 0.1$,[3] but compounds with x ranging up to 1 can be synthesized at high pressure and temperature.[4] Ca$_{0.86}$Sr$_{0.14}$CuO$_2$ has a tetragonal structure with lattice constants $a = 3.8611$ Å and $c = 3.1995$ Å, and contains no apical oxygen atoms. Simple valence counting yields a valence of +2 for the copper ions. The present system is the undoped parent compound of several cuprate superconductors having the same crystal structure; recently Azuma *et al.*[11] reported the synthesis of (Sr$_{1-x}$Ca$_x$)$_{1-y}$CuO$_2$ with T_c up to 110 K, and Smith *et al.*[12] obtained electron-doped IL superconductors (Sr$_{1-x}$Nd$_x$)$_{1-y}$CuO$_2$ and (Sr$_{1-x}$La$_x$)$_{1-y}$CuO$_2$ with $T_c \sim 50$ K.

Our specimen of Ca$_{0.86}$Sr$_{0.14}$CuO$_2$ was prepared by calcinating stoichiometric ratios of CaCO$_3$, SrCO$_3$, and CuO for 12 h in air. After several repetitions of calcination and regrinding, the powder was pressed into pellets

FIG. 2. Corrected asymmetry above and below the Néel temperature in Ca$_{0.86}$Sr$_{0.14}$CuO$_2$.

$Ca_{0.86}Sr_{0.14}CuO_2$
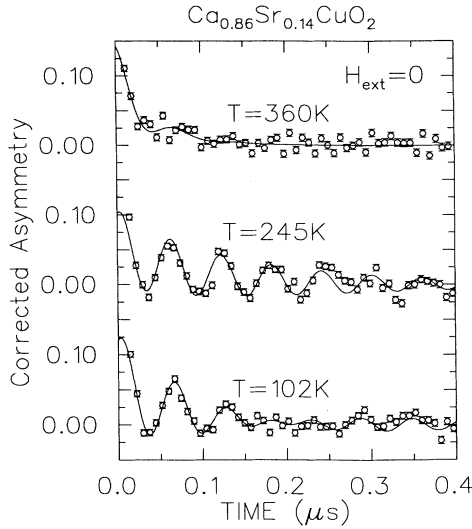

FIG. 3. Corrected asymmetry deep in the magnetically ordered state. The solid curves are fits to Eqs. (3) and (4) as described in the text.

$Ca_{0.86}Sr_{0.14}CuO_2$

FIG. 4. The temperature dependence of the muon-spin precision frequency in zero field along with neutron scattering data (Ref. 5) observed in $Ca_{0.86}Sr_{0.14}CuO_2$. Below 225 K two frequencies are seen. The solid lines are a power law $M(T) \propto (1 - T/T_N)^{0.26}$ and a molecular field curve. Fourier power spectra are shown in the inset.

cies into one. In that case some intermediate frequency will be measured when the hopping rate is much larger than the frequency at each site.[14] For further discussion of the two frequencies see Sec. IV B.

The μSR data below 300 K is analyzed with Eq. (3): We use two finite frequencies below 225 K and only one above 225 K. The high precession frequency indicates a strong local field due to the electronic moments, and the effect of nuclear moments becomes insignificant, as long as the determination of ν_μ is concerned. We therefore assume $\sigma = 0$ in the analysis at low temperatures. Since our data cannot resolve different spin-lattice relaxation times, we assume a single T_1 for the nonprecessing signal in our analysis. Unlike the frequency, the values obtained for T_1 were not well determined and depended on the details of the fitting scheme; therefore we do not present them here. The fitted asymmetry of the precessing component is approximately 44% of the total asymmetry; the difference from the ideal case of 2/3 may be ascribed to some nonprecessing background component and/or a possible missing precessing component having a very high frequency or relaxation rate. Figure 4 (solid circles) illustrates the temperature dependence of the muon precession frequency in $Ca_{0.86}Sr_{0.14}CuO_2$ normalized by 17.93 MHz. Below 225 K the curve splits into two lines centered around 16 MHz (H_{loc}=1.2 kG) with the higher frequency approaching 17.9(1) MHz [1.32(1) kG] and the lower frequency approaching 14.3 MHz [1.06(1) kG]. The precession frequencies depend only very weakly on the temperature below $0.5T_N$.

In most nonmetallic magnetic systems, the perturbation caused by the μ^+ to the magnetism of the host material is known to be minimal. We can expect the muon-spin precession frequency $\nu_\mu(T)$ to be proportional to the sublattice magnetization $M_s(T)$, as long as the muon site in the crystal is not altered. In neutron diffraction experiments, one measures the intensity of an antiferromagnetic Bragg peak, which is usually proportional to M_s^2
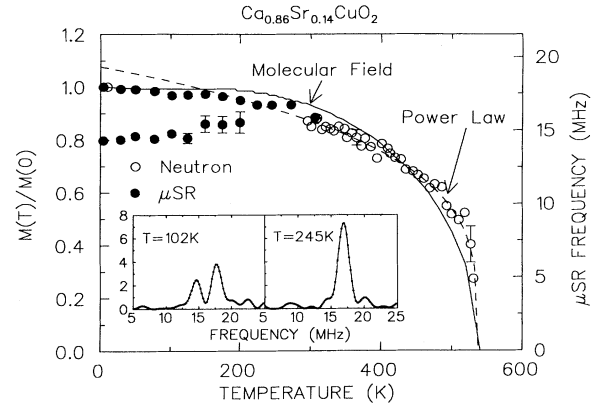
$(I_B \propto M_s^2)$. In Fig. 4 we also included the normalized $\sqrt{I_B}$ obtained by Vaknin et al.[15] The two magnetization curves match reasonably well in the intermediate temperature range. A power law $[M(T) \propto (1 - T/T_N)^{0.26}]$ and molecular field magnetization curves are also displayed: The former fits the results well only near T_N while the latter fits only at low temperatures.

IV. MUON DIFFUSION AND MUON SITE IN $Ca_{0.86}Sr_{0.14}CuO_2$

A. Muon diffusion

As shown in Fig. 3, the oscillations in the time spectra from $Ca_{0.86}Sr_{0.14}CuO_2$ start to disappear above 300 K, and are not observed at all at 400 K, even though a large static field ($B \sim 1$ kG) should exist at this temperature at the muon site. We attribute this strong dephasing of the muon-spin precession to muon hopping between sites of opposite magnetic field directions (due to the two sublattices in the ordered state of an antiferromagnet). In fact, such μ^+ hopping has been observed in the 1:2:3 system.[16] Equation (4) is used to fit the μSR time spectra between 306 K and 460 K assuming that the transverse relaxation caused by the hopping is much larger than any other sources of T_2. At 500 K and above, the relaxation is caused by the combination of hopping and the slowing down of the Cu spins in the critical regime. The relaxation behavior in this temperature range is beyond the scope of our model and is not discussed here.

The temperature dependence of the deduced hopping rate is shown in Fig. 5, where the results are compared with an Arrhenius law $\nu = \nu_0 \exp(-E_a/k_BT)$. The results agree reasonably with a straight line characterized by an activation energy $E_a = 0.39(1)$ eV and an asymptotic hopping rate $\nu_0 = 1.8(8) \times 10^{13}$ s^{-1}. These are the first quantitative results for muon diffusion and the
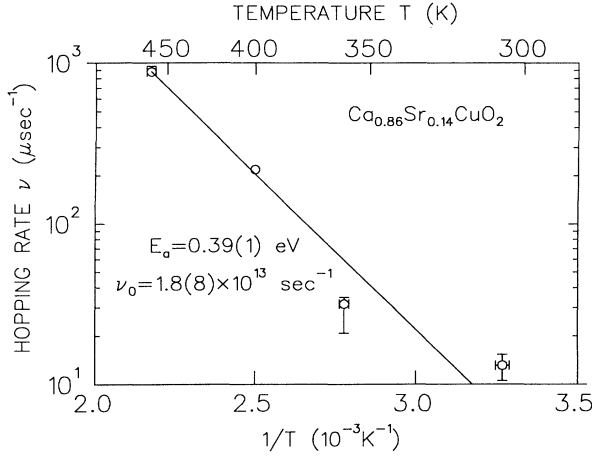
FIG. 5. Hopping rate as a function of temperature in $Ca_{0.86}Sr_{0.14}CuO_2$.

associated energy barrier in cuprates. The measured activation energy can be compared with the numerical calculation of the electrostatic potential in 1:2:3 systems by Li and Brewer.[17] According to their calculation, a muon trapped in a site between the two CuO_2 layers needs roughly 0.5 eV to escape from its site.

B. Muon sites

In the antiferromagnetic state of an insulator, we assume that the magnetic field seen by the muon is given by the dipolar field

$$H(\mathbf{R}_\mu) = \sum_i \frac{-\mu r_i^2 + 3(\boldsymbol{\mu} \cdot \mathbf{r}_i)\mathbf{r}_i}{|\mathbf{R}_\mu - \mathbf{r}_i|^5} , \qquad (5)$$

where $\mathbf{r}_i$ and $\mathbf{R}_\mu$ are the position of the ith Cu^{2+} ion and muon respectively, and $\boldsymbol{\mu}$ is the effective magnetic moment of the Cu^{2+} cation. Neutron scattering and susceptibility measurements[5] indicate that an effective moment of $0.51\mu_B$/Cu lies in the $\hat{\mathbf{a}}$-$\hat{\mathbf{b}}$ plane (in the ordered state of the IL). Here we assume that the moments make an angle of 45° with the $\hat{\mathbf{a}}$ axis in the $\hat{\mathbf{a}}$-$\hat{\mathbf{b}}$ plane, as was found in $LaCuO_4$ and $Sr_2CuO_2Cl_2$.[15] Since this moment does not involve any orbital component, the electrostatic interactions determining the muon site should not be different between the paramagnetic and ordered states. Then it is reasonable to assume that the muon site preserves the tetragonal symmetry of the crystal lattice. In contrast, the magnetic field in the cell has lower symmetry; i.e., the fields in two crystallographically equivalent sites are not necessarily equal.

To account for possible muon sites which could correspond to the two observed frequencies, we search for sites according to the restriction $H = 1.32(1)$ or $H = 1.06(1)$ kG, and obtain their coordinates (x, y, z) in the unit cell. Then the field for the crystallographically symmetric site $(x, b\text{-}y, z)$ is calculated. If the resulting field is either 1.32(1) or 1.06(1) kG, such a site is a candidate.

Otherwise, we should have seen a different frequency than the observed ones. There are two different types of sites: We refer to all sites where $H(x, y, z) = H(x, b\text{-}y, z)$ as type-A sites. There are two kinds of type-A site: A_{high} where $H = 1.32(1)$ and A_{low} where $H = 1.06(1)$ kG. If the muon occupies a type-A site we need to assume the existence of two crystallographically nonequivalent muon sites to obtain two frequencies. The other type is when $H(x, y, z)$ and $H(x, b\text{-}y, z)$ are not equal to each other, but one is 1.32(1) and the other is 1.06(1) kG. We call such a site type B. Only one crystallographic site of type B is needed in order to account for the two frequencies.

We performed a calculation of the local field in a lattice consisting of 8^3 unit cells, which gives an error in the calculated field comparable to the measured ones. A grid of 500^3 points is used to scan within the unit cell. Type-A sites are found only in the sides of the tetragon and in a plane passing through the Sr ion and midway between two adjacent Cu ions. Half of the $\hat{\mathbf{c}}$-$\hat{\mathbf{b}}$ plane and a plane passing through the Sr ion are plotted in Fig. 6(a). Since electrostatic arguments suggest that muon sites are roughly 1 Å away from an oxygen ion,[18] we highlighted this sphere by a solid line in the figure. We found A_{high} (solid circle) and A_{low} (open circle) sites roughly 1 Å away from the oxygen ion and very close to each other: The closest distance between A_{high} and A_{low} is 0.25 Å. If a muon stops randomly at either of these two type-A sites at low temperatures, two frequencies will be seen. One can then explain the merging of the two frequencies at elevated temperatures by assuming that the muon starts to hop from one site to the other.[14] In that case, the increase of the low frequency and the increase of the error bars of that frequency, as seen in Fig. 4, suggest that the site with low frequency is metastable.

We also found several type-B sites as shown in Fig. 6(b), which exist at a reasonable distance from an oxygen ion: The closest distance to oxygen is 1.25 Å. If the muon resides in any of these type-B sites at low temperatures a splitting of the frequency will be seen due to the lower symmetry of magnetic lattice. However, the measured ratio between the asymmetry of the high-frequency signal to the low-frequency signal is roughly 6 at low temperature. If the muon stops in a type-B site,
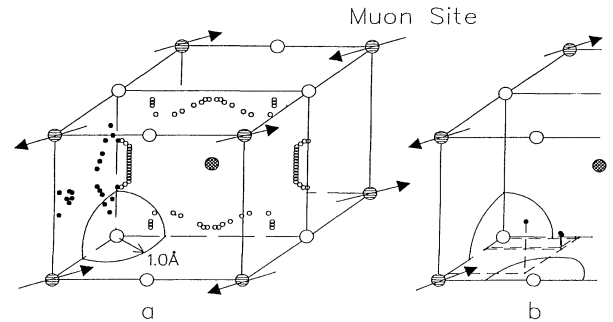

FIG. 6. Possible muon sites: (a) Only half of the $\hat{\mathbf{c}}$-$\hat{\mathbf{b}}$ plane and a plane passing through the Sr ion and between two Cu ions are plotted. On these planes, only type-A sites were found. (b) Type-B sites.

this ratio is expected to be 1. In addition, without rapid hopping between adjacent type-B sites, two frequencies are expected at any temperature. Hopping between two type-B sites is less likely because we would then expect a symmetric change in the frequency as the temperature increases, in contrast to the observed change. We therefore consider that the muon sites in $Ca_{0.86}Sr_{0.14}CuO_2$ are probably type-A sites.

V. μSR ON Sr_2CuO_3

The Sr_2CuO_3 sample was prepared by a similar sintering process as the $Ca_{0.86}Sr_{0.14}CuO_2$ sample. Powders of $SrCO_3$ and CuO were mixed with the ratio of 2:1 and were calcined at 960–970 °C for 12 h in air. The powder was then pressed into pellets and sintered at 1000°C for 12 h. The x-ray diffraction pattern was characterized by the peaks of the IC structure, except for several small unknown peaks with intensities less than 2.5% of the (011)-peak intensity.

In the orthorhombic structure of Sr_2CuO_3, the chains lie along the $\widehat{b}$ axis; there are no oxygen atoms between neighboring Cu atoms along the $\widehat{a}$ axis. The lattice constants are $a = 3.9122$ Å, $b = 3.4914$ Å, and $c = 12.7003$ Å. Each Cu atom is surrounded by four oxygen atoms: two from the chain and the other two from apical oxygen; see Fig. 1.[6] Valence counting gives +2 for the copper as in the IL case, and it is generally believed that this system is not doped with charge carriers.

Figure 7 shows μSR time spectra measured in Sr_2CuO_3. A large increase in the muon-spin depolarization occurs between $T = 6.0$ K and 5.5 K, which can be attributed to the slowing down of spin fluctuations, or to the appearance of a random static field. Muon-spin oscillations, indicating a static local field, appear only at 4.15 K and therefore the Néel temperature can be determined as $4.15 < T_N < 6$ K. This is consistent with the absence of magnon Raman scattering peaks in Sr_2CuO_3 at room temperature.[6] The μSR data was analyzed with Eq. (3), using two finite frequencies. The contribution to

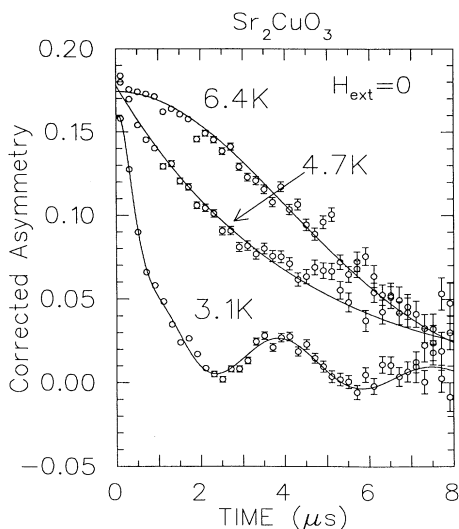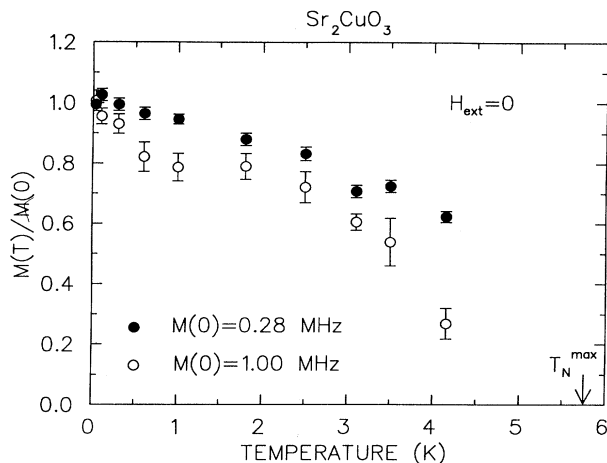FIG. 8. The temperature dependence of the muon-spin precision frequency in zero field, observed in Sr_2CuO_3.

the relaxation from nuclear moments was deduced from the high-temperature data and we assumed a single spin-lattice relaxation time. Here again we present only the frequencies since they are independent of the fitting procedure. The temperature dependence of the two observed frequencies is shown in Fig. 8. We see a fast reduction in the frequencies with increasing temperature, expected for the sublattice magnetization of a low-dimensional spin system.

Our results indicate that the magnetic order in Sr_2CuO_3 involves the majority of the sample volume. The observed oscillation signal is characteristic of uniform magnetic ordering, and quite different from the μSR signal in random spin systems such as spin glasses.[19] Therefore, we consider that the observed transition is due to the onset of CuO chain magnetic order and not due to a possible freezing of paramagnetic impurity spins.

VI. SUSCEPTIBILITY

Susceptibility measurements were made using a Quantum Design superconducting quantum interference device (SQUID) dc magnetometer with $H = 10$ kOe between 5 K and 400 K. The susceptibility data appearing in Fig. 9(a) were obtained after subtracting core diamagnetism and magnetic impurity contributions from the measured values; the magnetic impurity susceptibility was assumed to follow a Curie law. We also include measurements taken in $Sr_2CuCl_2O_4$ for comparison. The estimated magnetic impurity density, assuming Cu^{2+} impurities, is 0.026% in $Ca_{0.86}Sr_{0.14}CuO_2$, 0.25% in $S_2CuO_2Cl_2$, and 0.16% in Sr_2CuO_3. The impurity Curie term in Sr_2CuO_3 is sensitive to the annealing conditions: time, temperature, and atmosphere, as well as to sample age.[20] Some samples of Sr_2CuO_3 showed a Curie term corresponding up to a 3% impurity density.

The exchange interaction, within the CuO_2 planes in $Ca_{0.86}Sr_{0.14}CuO_2$ system, was estimated to be $J_{2D} \sim 1000$ K from the susceptibility measurement[5] and two-magnon Raman scattering.[13] This value is in agreement

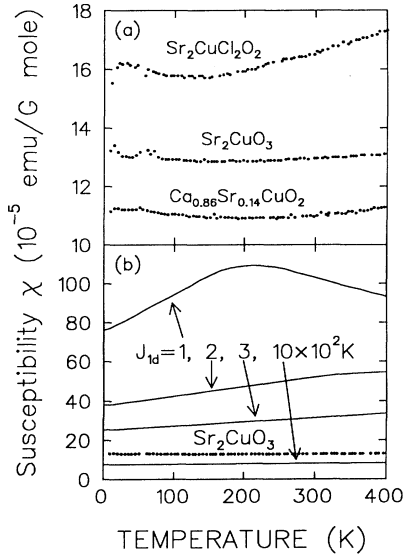FIG. 7. Corrected asymmetry above and below the Néel temperature in Sr_2CuO_3.

FIG. 9. Susceptibility measurements after the Curie and diamagnetic terms have been subtracted: (a) in layered compounds, and the infinite chain; (b) compared with the 1D model as described in the text.

FIG. 10. Comparison of $M(T)$ determined by μSR for compounds with three different layer separations. The solid lines represent a quasi-two-dimensional Heisenberg model. The parameter D is given by $D = g\mu_B H_A/4\bar{s}J$ where H_A is the anisotropy field.

with the J_{2D} of $La_{2-x}CuO_{4-y}$ determined from neutron scattering.[21] Since the expected Néel temperature within molecular field theory is ZJ, where Z is the nearest-neighbor coordination, T_N in this 2D system is suppressed by at most a factor of 10 from this value.

In Fig. 9(b), we compare the susceptibility measurement in Sr_2CuO_3 with a model calculation for the 1D Heisenberg spin chain consisting of $S = 1/2$ moments coupled antiferromagnetically, as given by Bonner and Fisher.[22] The model was solved numerically for the nearest-neighbor exchange interaction between N moments on a ring; the exact solutions for N ranging between 3 and 11 were extrapolated to $N \to \infty$. The temperature dependence of the dc susceptibility, for several values of the exchange interaction J_{1D}, is shown in the figure. It is clear that J_{1D} in Sr_2CuO_3 is on the order of 10^3 K, two orders of magnitude higher than the Néel temperature.

A large J_{1D} in Sr_2CuO_3 is also inferred from the formula $J \sim t_{pd}^4/\Delta^2 U$,[14] where t_{pd} is the O_{2p}-Cu_{3d} transfer integral and Δ and U are the charge transfer and onsite Coulomb energies. The charge transfer energy estimated from the optical absorption, $\Delta \sim 2.1$ eV,[6] is nearly the same as that of any parent insulator of the high-T_c cuprates. There is no reason to expect a much smaller t_{pd} in Sr_2CuO_3 compared with those in the other cuprates since the lattice constant is nearly identical. Therefore, J_{1D} in Sr_2CuO_3 should not be much different from J_{2D} for the CuO_2 planes in other cuprates.

VII. DISCUSSION

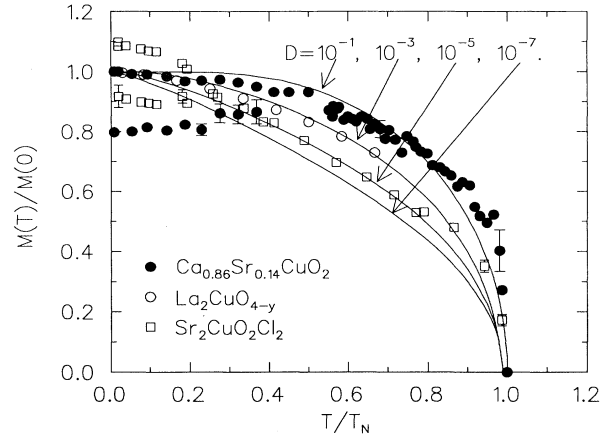Figure 10 shows the sublattice magnetization curves of three compounds, all containing CuO_2 plane layers, with different interlayer distance d_{CuO}: $Ca_{0.86}Sr_{0.14}CuO_2$ ($d_{CuO} = 3.1995$ Å), $La_2CuO_{4-0.015}$ ($d_{CuO} = 6.595$ Å) (Ref. 23), and $Sr_2CuO_2Cl_2$ ($d_{CuO} = 7.765$ Å)[24]. We see that the sublattice magnetization decreases most quickly with temperature when the interlayer separation is greatest. This can be attributed to a decrease in the effective dimensionality for systems with larger d_{CuO}. For antiferromagnetic spin waves with linear dispersion, the density of states is given as $n(\omega) \propto \omega^2$ in 3D systems, while $n(\omega) \propto \omega$ in 2D systems. Consequently, systems with lower dimensionality have a larger spectral weight of low-energy thermal magnon excitations. The sublattice magnetization is more easily destroyed by thermal excitations in 2D systems than in 3D systems. We see in Fig. 10 that increasing interlayer distance d_{CuO} takes the cuprate antiferromagnets closer to an ideal two-dimensional magnetic system (as one would expect).

To consider this behavior more quantitatively, we compare the experimental results with calculations for a simplified quasi-two-dimensional Heisenberg model previously studied by Lines.[25] It is known that ideal two-dimensional Heisenberg systems do not undergo magnetic order at finite temperatures. To account for the deviation from the 2D Heisenberg situation, this model introduces a uniaxial anisotropy field H_A which stabilizes the magnetic order. The Hamiltonian is then given by

$$\mathcal{H} = \sum_{NN} J\mathbf{S}_u \cdot \mathbf{S}_d - \sum_u g\mu_B H_A S_u^z + \sum_d g\mu_B H_A S_d^z \ , \quad (6)$$

where the subscript u (d) labels spins on "up" ("down") sites in the ordered phase, and the first summation runs over all nearest-neighbor spin pairs. The solution for $M(T)/M(0)$ was given by Lines[25], using a random-phase Green's function approximation. This solution depends on the parameter $D = g\mu_B H_A/4\bar{s}J$ which is proportional to the ratio of the anisotropy energy to the exchange energy. We calculated $M(T)/M(0)$ for various values of D, as described in Ref. 2 and show the results with the

solid lines in Fig. 10. The temperature dependence of the sublattice magnetization is very sensitive to the inclusion of a small anisotropy term: M decays very quickly with increasing T for small D values. We should note that, in the three cuprate systems mentioned above, the real mechanism for deviation from the ideal 2D Heisenberg interaction may be different from the uniaxial anisotropy assumed in the model Hamiltonian. In fact, an interlayer magnetic coupling, i.e., a small three-dimensional interaction, is more likely in our systems. Comparison of the model calculation and the observed results, however, allows us to roughly estimate the effective energy scale of the additional term to the ideal 2D Heisenberg interaction. Figure 10 demonstrates that an increasing interlayer distance d_{CuO} results in a very rapid reduction of such an additional anisotropy and/or a 3D term. This is quite reasonable if the 3D interlayer magnetic coupling plays a predominant role in the crossover from 3D to 2D behavior. Thus, $Ca_{0.86}Sr_{0.14}CuO_2$ is more appropriately described by a 3D model whereas $Sr_2CuO_2Cl_2$ is a very good example of a quasi-2D Heisenberg system.

In the infinite-chain system Sr_2CuO_3, the magnetic exchange interaction $J_{1D} \sim 1000$ K, inferred from uniform susceptibility measurements, is very high, while the present μSR study revealed that magnetic order occurs only below $T \sim 6$ K. The large ratio of $J_{1D}/kT_N \geq 100$ is quite remarkable: It is larger than those ratios in most of known prototypical 2D (Ref. 26) and 1D (Ref. 27) spin systems. This ratio indicates that the exchange interaction between the CuO chains is extremely small but finite. The μSR determination of T_N is completely unambiguous. On the other hand, there is a certain systematic ambiguity in the estimate of J_{1D} from uniform susceptibility, due to the subtraction of an impurity Curie term at low temperatures and a diamagnetic term at high temperatures. Therefore, it is important to estimate J_{1D} from more direct measurements, such as neutron scattering, when large single crystals become available.

The CuO chains in the 1:2:3 system $YBa_2Cu_3O_y$ have oxygen atoms missing for $y < 7.0$; complete chains exist only for $y = 7.0$. Furthermore, the CuO chain in the 1:2:3 system serves as a charge reservoir, and the average charge per Cu is often different from that of the Cu^{2+} ions in the insulating chains in Sr_2CuO_3. In $PrBa_2Cu_3O_7$, for example, Takenaka et al.[28] preformed an optical study and found that there are 0.5 holes per Cu in the CuO chain. The same number is expected in the CuO chain of $YBa_2Cu_3O_7$. Therefore, it is not appropriate to make a direct comparison between Sr_2CuO_3 and the CuO chains in the superconducting 1:2:3 systems.

On the other hand, there exist experimental results indicating that the chains in the 1:2:3 systems exhibit a quasi-one-dimensional nature. Two examples are (a) the low ordering temperature of the chain Cu moments; Li et al.[29] performed neutron scattering measurements in $NdBa_2Cu_3O_{6.35}$ and showed that the Cu moments in the CuO_2 planes order at $T_{N1} = 230$ K, while those in the CuO chain order at lower temperature $T_{N2} = 10$ K; (b) the tendency of holes, doped into the 1:2:3 chains, to be localized at low energy and low temperatures, as demonstrated[28] in $PrBa_2Cu_3O_7$. These features are most likely due to the geometrical structure of the CuO chains in these 1:2:3 compounds, characterized by the absence of oxygen atom between adjacent Cu atoms in the $\hat{a}$ direction. In this sense these 1:2:3 systems and Sr_2CuO_3 share a common origin for their quasi-1D behavior.

Sr_2CuO_3 could be a very interesting parent insulating system for charge-dopable CuO chains in 1:2:3 and possibly other cuprate systems. Detailed study of such systems could provide interesting results in testing theories for highly correlated 1D charge and spin chains, such as the 1D Hubbard model. In view of this, there is an ongoing effort to dope charge carriers in Sr_2CuO_3.[20] Another curious characteristic of Sr_2CuO_3 is the absence of a spin-Peierls state (due to the spin-phonon coupling) often observed in spin-1/2 1D systems,[30] including recently the 1D inorganic system $CuGeO_3$.[31]

In summary, we have performed μSR and susceptibility studies in the infinite-layer compound $(Ca,Sr)CuO_2$ and the infinite-chain system Sr_2CuO_3, and demonstrated that their magnetic behavior is deeply related to the low effective dimensionality of their magnetic interactions.

ACKNOWLEDGMENTS

APPENDIX

In a magnetically ordered sample, when temporal fluctuation and static spatial inhomogeneities are neglected, all muons that stop at the same site experience the same value of magnetic field. The polarization function in the z direction is described by

$$G_z(t) = g_0(t) = \text{Re}\left(\cos^2\theta + \sin^2\theta e^{i\omega(t-t_0)}\right) , \quad (A1)$$

where θ is the angle between the initial muon spin and the local field direction, and t_0 is the time the muon stops in the site.[9] However, at high temperatures we expect the muon to hop between sites. The effects of hopping are generally described within the framework of the strong collision model.[8] The term "strong collision" refers to the evolution of the local field experienced by the μ^+, which is assumed to change discontinuously at the time of a hop and to be uncorrelated with the evolution at the previous site.

In the strong collision model the muon is assumed to be hopping at random times between equivalent sites, with some average frequency ν_h. The time spent during a jump is taken to be much shorter than the mean residence

time at a site. The probability that the muon stays at a site after some period of time after its arrival is simply given by $e^{-\nu_h t}$.

The muon polarization at some time t will then contain contributions from muons that have not hopped at all, those that have hopped once, twice, and so on. After each

time the muon hops between sites of opposite magnetic fields the spin polarization starts to rotate in the opposite sense to the rotation before the hop. For n hops between sites of opposing field, at times $t_1 < \cdots < t_n < t$ ($t = t_{n+1}$), the polarization function g_n is given by

$$g_n(t_1, ..., t_n, t) = \mathrm{Re}\left[\cos^2(\theta) + \sin^2(\theta)\exp\left(i\sum_{i=1}^{n+1}(-1)^{i+1}\omega(t_i - t_{i-1})\right)\right] . \tag{A2}$$

If the probability of hopping between sites of opposite magnetic field per unit time is ν_h and if we sum over all possible number of hops, weighted by their probability, we get the familiar result[8]

$$G_z^h(t) = e^{-\nu_h t}g_0(t) + \nu_h\int_0^t dt_1 e^{-\nu_h t}g_1(t_1, t) + \nu_h^2\int_0^t dt_2\int_0^{t_2}dt_1 e^{-\nu_h t}g_2(t_1, t_2, t) + \cdots . \tag{A3}$$

In order to evaluate this sum we take the Laplace transform on both sides,

$$F(s) = \int_0^\infty e^{-st}G_z^h(t)dt. \tag{A4}$$

In this case the integrals in Eq. (A4) decouple and $F(s)$ is given by

$$F(s) = \mathrm{Re}\left(\cos^2\theta\sum_{n=1}\nu_h^{n-1}f_0^n(x) + \sin^2\theta f_\omega(x)[1 + \nu_h\overline{f_\omega}(x)]\sum_{n=0}\nu_h^n \mid f_\omega(x)\mid^n\right) , \tag{A5}$$

when $x = s + \nu_h$ and $f_\omega(x) = 1/(x - i\omega)$.

After summing over the geometrical sequences we get

$$F(s) = \cos^2\theta\frac{1}{s} + \sin^2\theta\left(\frac{c_+}{s - z_+} + \frac{c_-}{s - z_-}\right), \tag{A6}$$

where

$$c_\pm = \frac{1}{2} \pm \frac{\nu_h(\nu_h^2 - \omega^2)^{-\frac{1}{2}}}{2}$$

and

$$z_\pm = -\nu_h \pm (\nu_h^2 - \omega^2)^{\frac{1}{2}}.$$

$F(s)$ can be easily inverted to give

$$G_z^h(t) = \cos^2\theta + \sin^2\theta(c_+e^{z_+t} + c_-e^{z_-t}). \tag{A7}$$

In Fig. 11 we show $P_z(t)$ when $\nu_h > \omega$ and $\nu_h < \omega$. When $\nu_h > \omega$, the line shape is insensitive to the ratio ν_h/ω, and when $\nu_h < \omega$, the oscillations gradually disappear as $\nu_h \to \omega$. In the extreme cases the second term in Eq. (A7) can be written as a product of a relaxing part and an oscillating part. Taking the leading order in the oscillation frequency and relaxation we get

$$G_z^h(t) = \cos^2\theta + \sin^2\theta e^{-\frac{\omega}{2\nu_h}\omega t} , \qquad \nu_h \gg \omega , \tag{A8}$$

$$G_z^h(t) = \cos^2\theta + \sin^2\theta e^{-\nu_h t}\cos(\omega t) , \qquad \nu_h \ll \omega . \tag{A9}$$

In a powder sample we can replace the $\cos^2\theta$ with $\frac{1}{3}$ and the $\sin^2\theta$ with $\frac{2}{3}$ for the powder average.

If we include T_1 and T_2 relaxation from other sources, independent of the hopping, we arrive at

$$G_z^h(t) = \frac{1}{3}e^{-t/T_1} + \frac{2}{3}e^{-t/T_2}(c_+e^{z_+t} + c_-e^{z_-t}). \tag{A10}$$

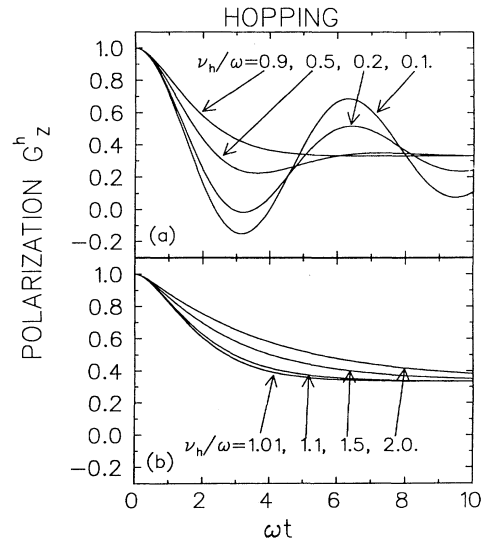This model is not applicable if the sizes of the magnetic

FIG. 11. Muon polarization along the beam direction for various ratios of hopping rate ν_h to rotation frequency ω calculated with the strong collision model. In (a) $\omega > \nu_h$ and in (b) $\omega < \nu_h$.

domains are smaller than the average length that the muon travels between sites or when the characteristic time of the field changes as seen by the muon in its flight is adiabatic with respect to $\gamma_\mu H$. It also should be noted

that hopping between sites of opposite fields ($\nu_h = \nu_{\uparrow\downarrow}$) is not the total hopping rate because hopping between sites of the same field ($\nu_{\uparrow\uparrow}$) also might occur; if ν_{tot} is the total hopping rate, then $\nu_{tot} = \nu_{\uparrow\downarrow} + \nu_{\uparrow\uparrow}$.

* Present address: Brookhaven National Laboratory, Upton, New York 11973.

[1] See, for example, papers published in *Proceedings of the International Conference on Materials and Mechanisms of Superconductivity High Temperature Superconductors II*, Stanford University, Stanford, CA (Elsevier Science Publishers B.V., North-Holland, 1989); Physica C **162-164**; *Proceedings of the International Conference on Materials and Mechanisms of Superconductivity High Temperature Superconductors III*, Kanazawa, Japan (Elsevier Science Publishers B.V., North-Holland, 1991); Physica C **185-189**.

[2] L. P. Le., G. M. Luke, B. J. Sternlieb, Y. J. Uemura, J. H. Brewer, T. M. Riseman, D. C. Johnston, and L. L. Miller, Phys. Rev. B **42**, 2182 (1990).

[3] T. Siegrist, S. M. Zahurak, D. W. Murphy, and R. S. Roth, Nature **334**, 231 (1988).

[4] M. Takano, Y. Takeda, H. Okada, M. Miyamoto, and T. Kusaka, Physica C **159**, 375 (1989).

[5] D. Vaknin, E. Caignol, P. K. Davies, J. E. Fischer, D. C. Johnston, and D. P. Goshorn, Phys. Rev. B **39**, 9122 (1989).

[6] M. Yoshida, S. Tajima, N. Koshizuka, and S. Tanaka, Phys. Rev. B **44**, 11 997 (1991).

[7] Y. J. Uemura, W. J. Kossler, J. R. Kempton, X. H. Yu, H. E. Schone, D. Opie, C. E. Stronach, J. H. Brewer, R. F. Kiefl, S. R. Kreitsman, G. M. Luke, T. Riseman, K. Ll. Williams, E. J. Ansaldo, Y. Endoh, K. Kudo, K. Yamada, D. C. Johnston, M. Alvarez, D. P. Goshorn, Y. Hidaka, M. Oda, Y. Enomoto, M. Suzuki, and T. Murakame, Physica C **153-155**, 769 (1988); Y. J. Uemura, W. J. Kossler, X. H. Yu, J. R. Kempton, H. E. Schone, D. Opie, D. C. Johnston, M. S. Alvarez, and D. P. Goshorn, Phys. Rev. Lett. **59**, 1045 (1987).

[8] R. S. Hayano, Y. J. Uemura, J. Imazato, N. Nishida, T. Yamazaki, and R. Kubo, Phys. Rev. B **20**, 850 (1979); Y. J. Uemura, Master's thesis, University of Tokyo, 1979.

[9] A. Schenck, *Muon Spin Rotation Spectroscopy: Principles and Application in Solid State Physics* (Hilger, Bristol, 1986).

[10] R. S. Roth (unpublished).

[11] M. Azuma, Z. Hiroi, M. Takano, Y. Bando, and Y. Takeda, Nature **356**, 775 (1992).

[12] M. G. Smith, A. Manthiram, J. Shou, J. B. Goodenough, and J. T. Markert, Nature **351**, 549 (1991).

[13] Y. Tokura, S. Koshihara, T. Arima, H. Takagi, S. Ishibashi, T. Ido, and S. Uchida, Phys. Rev. B **41**, 11 657 (1990).

[14] A. Abragam, *Principles of Nuclear Magnetism* (Oxford University Press, New York, 1961); C. P. Slichter, *Principles of Magnetic Resonance* (Springer-Verlag, Berlin, 1978).

[15] D. Vaknin, S. K. Sinha, C. Stassis, L. L. Miller, and D. C. Johnston, Phys. Rev. B **41**, 1926 (1990).

[16] R. F. Kiefl, J. H. Brewer, I. Affleck, J. F. Carolan, P. Dosanjh, W. N. Hardy, T. Hsu, P. Kadone, J. R. Kempton, S. R. Kreitzman, Q. Li, A. H. O'Reilly, T. M. Riseman, P. Schleger, P. C. E. Stamp, L. P. Le, G. M. Luke, B. Stermlieb, Y. J. Uemura, H. R. Hart, and K. W. Lay, Phys. Rev. Lett. **64**, 2082 (1990).

[17] Q. Li and J. H. Brewer, Hyperfine Interact. **63**, 169 (1991).

[18] W. K. Dawson, K. Tibbs, S. P. Weathersby, C. Boekema, and K.-C. B. Chan, J. Appl. Phys. **64**, 5890 (1988).

[19] Y. J. Uemura, T. Yamasaki, D. R. Harshman, M. Senba, and E. J. Ansaldo, Phys. Rev. B **31**, 546 (1985).

[20] M. Crawford and T. Ami (private communication).

[21] G. Shirane, Y. Endoh, R. J. Birgeneau, M. A. Kastner, Y. Hidaka, M. Oda, M. Suzuki, and T. Murakami, Phys. Rev. Lett. **59**, 1613 (1987).

[22] J. C. Bonner and M. E. Fisher, Phys. Rev. **135**, A640 (1964).

[23] B. Y. Yand, S. Mitsuda, G. Shirane, Y. Yamaguchi, H. Yamauchi, and Y. Syono, J. Phys. Soc. Jpn. **56**, 2283 (1987).

[24] L. L. Miller, X. L. Wand, S. X. Wand, C. Stassis, D. C. Johnston, J. Faber, Jr., and C.-K. Loong, Phys. Rev. B **41**, 1921 (1990).

[25] M. E. Lines, J. Phys. Chem. Solids **31**, 101 (1970).

[26] L. J. de Jonge and A. R. Miedama, Adv. Mod. Phys. **23**, 1 (1974).

[27] M. Steiner, J. Villain, and C. G. Windsor, Adv. Phys. **25**, 87 (1976).

[28] K. Takenaka, Y. Imanaka, K. Tamasaku, T. Ito, and S. Uchida, Phys. Rev. B **46**, 5833 (1992).

[29] W-H. Li, J. W. Lynn, and Z. Fisk, Phys. Rev. B **41**, 4098 (1990).

[30] I. S. Jacobs, J. W. Bary, H. R. Hart, Jr., L. V. Interrante, J. S. Kasper, G. D. Watkins, D. E. Prober, and J. C. Bonner, Phys. Rev. B **14**, 3036 (1976).

[31] M. Hase, I. Terasaki, and K. Uchinokura, Phys. Rev. Lett. **70**, 3651 (1993).